



Published in final edited form as:

*Clin Oral Investig.* 2018 April ; 22(3): 1243–1252. doi:10.1007/s00784-017-2215-y.

## Doxycycline-loaded nanotube-modified adhesives inhibit MMP in a dose-dependent fashion

Jadesada Palasuk<sup>1,2</sup>, L. Jack Windsor<sup>2</sup>, Jeffrey A. Platt<sup>2</sup>, Yuri Lvov<sup>3</sup>, Saulo Geraldeli<sup>4</sup>, and Marco C. Bottino<sup>5,\*</sup>

<sup>1</sup>Department of Restorative Dentistry, Faculty of Dentistry, Naresuan University, Phitsanulok, 65000, Thailand <sup>2</sup>Department of Biomedical and Applied Sciences, Indiana University School of Dentistry, Indianapolis, IN, 46202, USA <sup>3</sup>Institute for Micromanufacturing, Louisiana Tech University, Ruston, LA, 71272, USA <sup>4</sup>Department of Restorative Dental Sciences, Operative Division, College of Dentistry, University of Florida, Gainesville, FL, 32610, USA <sup>5</sup>Department of Cariology, Restorative Sciences, and Endodontics, University of Michigan School of Dentistry, Ann Arbor, MI, 48109, USA

### Abstract

**Objectives**—This article evaluated the drug loading, release kinetics, and matrix metalloproteinase (MMP) inhibition of doxycycline (DOX) released from DOX-loaded nanotube-modified adhesives. DOX was chosen as the model drug, since it is the only MMP inhibitor approved by the U.S. Food and Drug Administration.

**Materials and methods**—Drug loading into the nanotubes was accomplished using DOX solution at distinct concentrations. Increased concentrations of DOX significantly improved the amount of loaded DOX. The modified adhesives were fabricated by incorporating DOX-loaded nanotubes into the adhesive resin of a commercial product. The degree of conversion (DC), Knoop microhardness, DOX release kinetics, antimicrobial, cytocompatibility, and anti-MMP activity of the modified adhesives were investigated.

**Results**—Incorporation of DOX-loaded nanotubes did not compromise DC, Knoop microhardness, or cell compatibility. Higher concentrations of DOX led to an increase in DOX release in a concentration-dependent manner from the modified adhesives. DOX released from the modified adhesives did not inhibit the growth of caries-related bacteria, but more importantly it did inhibit MMP-1 activity.

**Conclusions**—The loading of DOX into the nanotube-modified adhesives did not compromise the physicochemical properties of the adhesives and the released levels of DOX were able to inhibit MMP activity without cytotoxicity.

\* **Corresponding author:** Dr. Marco C. Bottino, University of Michigan, School of Dentistry, Department of Cariology, Restorative Sciences and Endodontics, 1011 N. University Avenue, Ann Arbor, MI, 48109, USA, Tel: +1-734-763-2206; fax: +1-734-936-1597. mbottino@umich.edu (M.C. Bottino).

**Compliance with Ethical Standards**

**Ethical Approval** This article does not contain any studies with human participants or animals performed by any of the authors.

**Informed Consent** Not applicable.

**Conflict of Interest** The authors declare that they have no conflict of interest.

**Clinical significance**—Doxycycline released from the nanotube-modified adhesives inhibited MMP activity in a concentration-dependent fashion. Therefore, the proposed nanotube-modified adhesive may hold clinical potential as a strategy to preserve resin/dentin bond stability.

### Keywords

dental adhesive; matrix metalloproteinase; Halloysite<sup>®</sup>; doxycycline; nanotubes

---

### Introduction

Over the past decade, resin composites have become the material of choice for direct restoration of teeth compromised by dental caries due to their aesthetic properties and minimally-invasive cavity preparations [1]. However, resin composite restorations have an average lifetime of only 5.7 years [2]. Secondary caries that develops at the interface between resin composite restoration and dental tissue (dentin/enamel) is the primary reason for restoration replacement [3].

Although the field of adhesive dentistry has greatly evolved over the years, the basic principles of bonding to tooth structure remain unchanged. It is critical to achieve a micromechanical interlocking (adhesive resin/tooth structure) to obtain a stable and durable bond [4]. This process has been termed “hybridization” or the formation of the hybrid layer [5]. The hybrid layer (HL) is the zone where resin monomers flow and polymerize into acid-etched dentin to establish micromechanical interlocking with the demineralized collagen matrix. Unfortunately, sub-optimal resin monomer infiltration leaves behind a denuded collagen matrix susceptible to endogenous protease activity (i.e., matrix metalloproteinases/MMPs and cathepsins) that will digest the unprotected collagen and deteriorate the HL over time [2, 6] and may contribute to the secondary caries formation.

In recent years, several strategies including the use of MMP inhibitors [7, 8] and chelating agents (e.g., chlorhexidine) [9, 10] have been suggested to counteract and/or inhibit the activity of MMPs and cathepsins. Yet, the levels of MMPs and/or cathepsins inhibition and associated bond stability was not sustained after long-term (>18 months) aging [10, 11]. Taken together, these findings strongly highlight the pressing need to discover a clinically-translatable strategy that would support a localized and sustained release of MMP and/or cathepsin inhibitors.

Aluminosilicate (Halloysite<sup>®</sup>, HNT) is a naturally-occurring tubular clay formed by rolled kaolin with a general length between 500–1500 nm [12]. Interestingly, the inner surface of HNT has chemical properties similar to those of Al<sub>2</sub>O<sub>3</sub> as it is formed by the octahedral sheet of Al–OH, while the outer surface has chemical properties identical to those of SiO<sub>2</sub> resulting from siloxane groups (Si–O–Si) [12]. This difference in chemical composition results in a negatively charged outer surface and a positively charged inner lumen approximately 10–15 nm in diameter [12]. With this as the goal, our group recently started to report on a novel strategy of modifying dental adhesives with these clay nanotubes [13–16] to deliver MMP inhibitors (e.g., DOX) at the HL level to enhance resin-dentin bond durability. Our seminal proof-of-concept data clearly demonstrated e inhibition of MMP-1 activity by eluates obtained from DOX-loaded nanotube-modified adhesives when testing

the effects of a 10% (w/v) doxycycline solution [14]. Our previous work lacks detailed information on the release kinetics, and concentration range of loaded DOX, since the MMP inhibition by the DOX eluate was 13.4%. The aim of this study was to further evaluate the loading potential and MMP-inhibiting effects of different concentrations of DOX-loaded nanotube-modified dental adhesives by including thorough high performance liquid chromatography (HPLC/mass spectroscopy) analyses to appreciate the drug loading potential and release kinetics. We hypothesized that increased concentrations of DOX would not compromise physico-chemical of the modified adhesive and would show higher release of DOX and MMP inhibition without toxicity.

## Materials and methods

### Preparation of doxycycline solutions and nanotube loading

Doxycycline hyclate (DOX, Sigma-Aldrich, St. Louis, MO, USA) was dissolved in 5 mL of 50 mM HEPES buffer (pH = 7.2, Fisher Scientific, Pittsburgh, PA, USA) at three distinct concentrations (w/v): 10% (0.5 g), 20% (1 g), and 30% (1.5 g) by stirring (Fisher Thermix, model 310T, Fisher Scientific). The loading process started by mixing a predetermined amount (1.25 g) of pre-sieved (<45  $\mu\text{m}$ ) Halloysite<sup>®</sup> nanotubes (HNT, Dragonite 1415JM, Applied Minerals Inc., New York, NY, USA) in 5 mL of each DOX solution and followed by sonication for 2 h [19]. In order to minimize any air between and within the nanotubes, the solutions were placed in a vacuum (25 in.Hg) chamber for 1 h. Next, the solutions were mixed for 1 h and vacuum was reapplied [14]. Finally, the HNT+DOX solutions were centrifuged (3000 rpm) for 10 min. The supernatants were collected and stored at  $-20^{\circ}\text{C}$  for high-pressure liquid chromatography (HPLC) analysis. Meanwhile, the HNT+DOX pellets were dried at  $37^{\circ}\text{C}$ , weighed, ground, and sieved.

### Loading efficiency and drug loading

The amount of DOX in the supernatants (SUPs) after the loading process was assayed by HPLC (1100 Series, Agilent Technologies, Palo Alto, CA, USA) equipped with a UV-Vis detector. An Eclipse XDB-C18 (Agilent Technologies) chromatography column (3.5  $\mu\text{m}$ ,  $150 \times 4.6$  mm) and 10  $\mu\text{L}$  injection volume were used. A binary mobile phase consisting of solvent systems A and B was used in an isocratic elution with 80:20 A:B. Mobile phase A was 50 mM  $\text{KHPO}_4$  in  $\text{dH}_2\text{O}$  and mobile phase B was 100% acetonitrile. The HPLC flow rate was 1.0 mL/min and the total run time was 10 min. The retention time was 4.85 min. The concentration of DOX was calculated based on a standard curve of known levels of DOX at 273 nm. The amount of un-loaded and loaded DOX was calculated as follows:

$$\text{Un-loaded DOX (mg)} = \text{conc. of DOX in SUP (mg/mL)} \times \text{vol. of SUP (mL)}$$

$$\text{Loaded DOX (mg)} = \text{Amount of DOX added (mg)} - \text{un-loaded DOX (mg)}$$

Loading efficiency and drug loading were obtained using the equations [17]:

$$\text{Loading efficiency (\%)} = \frac{D_a - D_s}{D_a} \times 100$$

$$\text{Drug loading (\%)} = \frac{D_a - D_s}{N_a} \times 100$$

Where:  $D_a$  = total DOX added (g),  $D_s$  = un-loaded DOX (g), and  $N_a$  = total HNT (1.25 g)

### Doxycycline-loaded nanotube-modified dental adhesive fabrication

The experimental adhesives were prepared by mixing using a stirrer and conical micropestle [13–16]. DOX-loaded (10%, 20%, and 30% DOX) nanotubes were added to a commercially available adhesive (Adper Scotchbond Multi-Purpose [SBMP], 3M ESPE, St. Paul, MN, USA) at 15% (w/v, 75 mg of HNT+DOX in 500  $\mu$ L of adhesive) and sonicated to enhance HNT dispersion [13–16]. Foil-covered light-proof (amber) microcentrifuge tubes were used during the fabrication process due to DOX photosensitivity [18]. Control groups consisting of unmodified adhesive (SBMP) and DOX-free nanotube modified adhesives were also fabricated. All specimens were prepared in a constant-temperature room (23°C) equipped with a filtered lighting system to lessen inadvertent polymerization.

### Degree of conversion (DC)

Adhesive disks ( $7 \times 0.24$  mm,  $n = 5/\text{group}$ ) were fabricated with a Teflon<sup>®</sup> mold by adhesive resin light-curing using a light-emitting diode curing unit (DEMI LED, Kerr, Orange, CA, USA). The amounts of energy applied to the specimens during light-curing for 10, 20, and 40 s, as measured with a MARC Resin Calibrator (BlueLight analytics Inc., Halifax, NS, Canada) were 10.92 J/cm<sup>2</sup>, 22.49 J/cm<sup>2</sup>, and 46.18 J/cm<sup>2</sup>, respectively. DC was evaluated with Fourier transform infrared spectroscopy (FTIR, Jasco 4100, JASCO Corporation, Tokyo, Japan) in attenuated total reflection mode. The areas under 2 absorbance bands at 1,637 cm<sup>-1</sup> (methacrylate C=C) and 1,715 cm<sup>-1</sup> (ester C=O) were recorded [13, 16]. DC was calculated using the following equation:

$$\text{DC (\%)} = \left(1 - \frac{\text{Cured (area under } 1637 \text{ cm}^{-1} / \text{area under } 1715 \text{ cm}^{-1})}{\text{Uncured (area under } 1637 \text{ cm}^{-1} / \text{area under } 1715 \text{ cm}^{-1})}\right) \times 100$$

### Knoop microhardness

Five disk-shaped ( $6.2 \times 1.0$  mm,  $n=5/\text{group}$ ) adhesive specimens were prepared by light-curing (20 s/side) for Knoop microhardness analyses. The specimens were then mounted in self-cure epoxy resin (EpoxiCure<sup>®</sup>, Buehler, Lake Bluff, IL, USA) and finished with 1200-grit SiC paper (Buehler). The specimens were subjected to a microhardness test (M-400, LECO Corporation, St. Joseph, MI, USA) using a Knoop diamond indenter at a 50 gf load and 15 s dwell time [13]. Five readings at different locations were taken from each specimen. The long diagonal length was measured immediately and converted to a KHN

number ( $\text{kg}/\text{mm}^2$ ). The adhesive specimens used for the assays described below were fabricated following this protocol.

### Drug release profile from DOX-loaded nanotube-modified dental adhesives

Disk-shaped specimens ( $n=6/\text{group}$ ) were fabricated and individually incubated at  $37^\circ\text{C}$  in 1 mL of phosphate buffer saline (PBS, pH 7.4, Fisher Scientific). Then, 150  $\mu\text{L}$  aliquots (PBS eluates) were collected after 1, 7, 14, 21, and 28 days. An equal volume of fresh PBS was added back to keep the volume constant. Aliquots were stored at  $-20^\circ\text{C}$  until used for high performance liquid chromatography tandem mass spectrometry (HPLC-MS-MS, Agilent 6460 Triple Quadrupole LC/MS, San Jose, CA, USA). The analysis was performed using an XBridge-C18 chromatography column ( $3.5 \mu\text{m}$ ,  $100 \times 2.1 \text{ mm}$ ) with a 5  $\mu\text{L}$  injection volume. The mobile phase consisted of 0.1% formic acid in deionized water (A) and 0.1% formic acid in acetonitrile (B) under an isocratic condition (A:B, 80:20). A flow rate of 0.30 mL/min was used. The mass spectrometer was operated in multi-reaction monitoring (MRM) mode. The transition for doxycycline was mass:charge ( $m/z$ ) at 445.1 (MS1) and 428.1 (MS2). The concentration of released DOX was calculated based on a standard curve prepared for DOX solution at known concentrations ( $r^2 = 0.99986$ ).

### DOX content in the nanotube-modified dental adhesive and after long-term storage

The total DOX content in the freshly prepared adhesive disks ( $n=4/\text{group}$ ) and after 4 months of storage in PBS at  $37^\circ\text{C}$  was determined by dissolving the specimens in dimethyl sulfoxide (DMSO, Fisher Scientific). Next, the solubilized DOX-containing adhesive/DMSO solutions were centrifuged (4000 rpm) and the supernatants were collected and stored at  $-20^\circ\text{C}$  until analyzed by mass spectrometry. The overall outcomes were to determine (1) the total amount of DOX that was incorporated into the adhesive specimens and (2) the amount of DOX remaining in each specimen after 4 months.

### Antimicrobial properties of DOX-loaded nanotube-modified dental adhesives

Disk-shaped specimens ( $n=3/\text{group}$ ) were fabricated and disinfected by ultraviolet (UV) irradiation (30 min/side) for antimicrobial analyses [14]. *Streptococcus mutans* (*S. mutans*, UA159) and *Lactobacilli casei* (*L. casei*, ATCC 393) were cultured aerobically in tryptic soy broth (Difco Laboratories, Detroit, MI, USA) for 24 h in 5%  $\text{CO}_2$  at  $37^\circ\text{C}$ . Then, 100  $\mu\text{L}$  of the bacterial suspension was swabbed onto blood agar plates to individually create lawns of the selected bacteria [14, 19]. The agar plates were divided into zones and adhesive disks or 10  $\mu\text{L}$  of previously collected eluates were placed onto the plates (bioMérieux, Inc., Durham, NC, USA) [14]. The blood agar plates were incubated in 5%  $\text{CO}_2$  at  $37^\circ\text{C}$ . After 72 h, the inhibition zones (mm) were measured. Chlorhexidine (0.12%) and sterile PBS were used as the positive and negative controls, respectively.

### Cytocompatibility

UV-disinfected, disk-shaped specimens ( $n=4/\text{group}$ ) were used to prepare eluates from the adhesives, according to the guidelines of the International Standards Organization (1993) [20]. The specimens were individually soaked in 15 mL of low glucose Dulbecco's Modified Eagle's Medium (DMEM, Gibco, Grand Island, NY, USA) supplemented with 10% FBS

(HyClone, Logan, UT, USA) and 1% penicillin–streptomycin (Sigma-Aldrich). The eluate extraction was performed at 37°C (24 h) under agitation. Next, the eluates were serially diluted to 32-fold, 64-fold, and 128-fold [21]. Human dental pulp stem cells (hDPSCs, AllCells LLC, Alameda, CA, USA) were cultured under standard conditions in a humidifier incubator (5% CO<sub>2</sub>/95% air) at 37°C in low-glucose DMEM supplemented with 10% FBS (HyClone) and 1% penicillin–streptomycin (Sigma). Cytotoxicity was performed as previously described [14] using WST-1 assay (Roche Diagnostics, Indianapolis, IN, USA) according to the manufacturer's instructions. Cell viability data (% , mean ± SD) are presented as determined from the ratio of experimental value to value from untreated cells.

### **Anti-MMP activity of DOX-loaded nanotube-modified dental adhesives**

The anti-MMP activity of DOX-loaded nanotube-modified adhesives was determined by testing eluates collected in Trishydroxymethylaminomethane (Tris) buffer over 28 days using a fluorescein isothiocyanate (FITC)-labeled type I collagen cleavage assay.

### **Eluate preparation from DOX-loaded nanotube-modified dental adhesives**

Disk-shaped specimens (n=4/group) were fabricated as previously described and used to prepare eluates from the experimental adhesives and controls (i.e., SBMP and DOX-free nanotube-modified adhesive). The specimens were individually incubated at 37°C in 1 mL of Tris buffer (pH=7.4, 50 mM Tris-HCl, 0.2 M NaCl, 5 mM CaCl<sub>2</sub>, 1 μM ZnCl<sub>2</sub>, and 15 mM NaN<sub>3</sub>). Aliquots (150 μL) were retrieved at days 1, 7, 14, 21, and 28. An equal volume of buffer was added to keep the extraction volume constant. Aliquots were stored at –20°C until use.

### **FITC labeled type I collagen cleavage assay**

Type I collagen derived from rat-tail tendon (RTT) was purified and labeled with fluorescein isothiocyanate (FITC, Sigma-Aldrich) [22]. Human pro-matrix metalloproteinase 1 (pro-MMP-1, 0.05 mg/mL, Abcam, Cambridge, MA, USA) was activated with 4-aminophenylmercuric acetate (APMA, Sigma-Aldrich) [23]. Successful activation was confirmed using western blot analysis [24]. All the eluates (150 μL, n=4/group) collected from the fabricated adhesives in Tris buffer were incubated with APMA activated MMP-1 for 30 min at RT. Then, Tris buffer (200 μL) and FITC-labeled type I collagen (50 μL) were added and the mixture was incubated at 37°C for 120 min. The negative and positive controls for the assay were Tris buffer and a 0.1% DOX solution, respectively. Samples (70 μL) were periodically (0–120 min) removed and the reaction was terminated by the addition of 1,10-phenanthroline (200 mM, 10 μL) to a final concentration of 25 mM [28]. Reducing SDS-PAGE sample buffer was added (1:1), samples boiled for 10 min, and then resolved in 8% SDS-PAGE (150 V, 3 h). The fluorescent signals were captured using the Bio-Rad imaging system (Gel Doc™ XR imaging system). The fluorescence intensity at 0 min and 120 min incubation was analyzed with ImageJ software (National Institutes of Health, Bethesda, MD, USA). The percent of FITC labeled RTT of buffer, 0.1% DOX (positive control), and eluate collected from the adhesives was calculated as follows [22]:

$$\text{Cleaved RTT (\%)} = \left(1 - \frac{\text{Fluorescent density at 2h}}{\text{Fluorescent density at 0h}}\right) \times 100$$

The percent (%) of MMP inhibition was calculated using the following equation:

$$\text{Inhibition (\%)} = \frac{\text{Cleaved RTT in buffer (\%)} - \text{cleaved RTT of eluates (\%)}}{\text{Cleaved RTT in buffer (\%)}} \times 100$$

### Transmission electron microscopy (TEM)

TEM analysis was carried out on resin composite/HNT-modified experimental adhesive samples in order to confirm the presence of the nanotubes (HNTs) within the adhesive resin. Resin composite/SBMP specimens were also prepared for comparison purposes. Disk-shaped specimens (7 × 2 mm) were fabricated using a custom-made silicone mold (Exaflex Putty, GC America Inc., Alsip, IL, USA). Next, resin composite (RC, Durafill VS shade A2, Heraeus Kulzer GmbH, Dirmagen, Germany) was placed into the mold and cured for 40 s, followed by application of the nanotube-modified adhesive (DOX-free) and light-curing for 20 s. Likewise, the control specimens were prepared using the SBMP adhesive resin. The specimens were cut to produce approximately 2 × 2 × 2 mm<sup>2</sup> beams using a diamond disk before TEM preparation [25]. Ultra-thin sections (70–90 nm) were taken from the resin blocks containing the RC/adhesive samples using a diamond knife (Diatome, Electron Microscopy Sciences, Hatfield, PA, USA), placed on copper mesh grids and then imaged at 80 kV (TEM, Tecnai BioTWIN, FEI, Hillsboro, OR, USA).

### Statistical analysis

The data were analyzed using one-way Analysis of Variance (ANOVA) followed by Tukey's test for multiple comparisons. A significance level was set at  $\alpha=0.05$ .

## Results

### Loading efficiency and drug loading

Statistical analyses revealed significant ( $p<0.001$ ) differences in the amount of loaded DOX, loading efficiency, and drug loading among the three groups (Table 1). Overall, increases in the concentration of DOX significantly increased the amount of DOX that was loaded into the HNTs. Meanwhile, increases in the concentration of DOX significantly decreased loading efficiency.

### Degree of conversion (DC)

DC data for the control (SBMP) and modified adhesives polymerized for 10, 20, or 40 s are shown in Figure 1. Increasing curing times led to an increase in the DC: 61.40–64.68 % (10 s), 64.15–68.65 % (20 s), and 70.44–73.26 % (40 s). No significant differences were found with each curing time among the modified adhesives and the control (SBMP,  $p > 0.05$ ).

### **Knoop microhardness**

The Knoop microhardness values for the adhesives tested are shown in Figure 2. There were no significant ( $p > 0.05$ ) differences between the nanotube-modified dental adhesives (with or without DOX) when compared to the control (SBMP).

### **Drug release profile from DOX-loaded nanotube-modified dental adhesives**

An initial burst release was seen at day 1 and followed by a gradual decrease over time (Figure 3). The cumulative release of DOX (mean  $\pm$  SE) from the adhesive over 28 days was  $4.04 \pm 0.05$   $\mu\text{g}$  (10% DOX),  $4.79 \pm 0.07$   $\mu\text{g}$  (20% DOX), and  $8.21 \pm 0.088$   $\mu\text{g}$  (30% DOX). No significant differences in the DOX cumulative release were found among the groups ( $p = 0.259$ ).

### **DOX content in the nanotube-modified dental adhesive and after long-term storage**

When specimen disks were dissolved in DMSO, the total DOX content in the adhesive disks ranged from 292.51–1644.17  $\mu\text{g}$  (10–30%DOX). After long-term storage (4 months), the amount of DOX in the adhesive disks decreased to as low as 39.77  $\mu\text{g}$  (10% DOX). The percent (%) remaining in the adhesive disks was 13.60 (10% DOX), 6.09 (20% DOX), and 6.24 (30% DOX), when compared to the original amount of DOX present in the dental adhesives.

### **Antimicrobial properties**

Representative photographs shown in Figure 4 demonstrate significant growth inhibition of *S. mutans* and *L. casei*. The inhibition zones for both bacteria when in contact with the DOX-loaded nanotube-modified adhesives were seen as a function of the amount of DOX within the adhesives. Statistical analysis showed that inhibition zones for *S. mutans* and *L. casei* were significant among the three groups, except for the inhibition zone of *L. casei*, which was between 10%DOX and 20%DOX.

### **Cytocompatibility**

Figure 5 shows hDPSC viability (%) following exposure to eluates collected from the experimental adhesives and the control. No significant differences ( $p > 0.05$ ) were found among cells incubated with eluates, at the same dilution, for each adhesive when compared with the control group (i.e., cells that were not incubated with eluate, 100% survival).

### **Anti-MMP activity of DOX-containing eluates**

FITC-labeled type I collagen cleavage assay demonstrated significant MMP-1 inhibition by DOX-containing eluates (Figure 6). Day 1 eluates led to the highest MMP-1 inhibition [ $16.20 \pm 8.09\%$  (10% DOX),  $23.61 \pm 3.33\%$  (20% DOX), and  $26.33 \pm 5.01\%$  (30% DOX)], followed by a gradual decrease over time. No significant differences in MMP-1 inhibition were found among the 10%, 20%, and 30% DOX groups ( $p > 0.05$ ).

### **Transmission electron microscopy (TEM)**

Representative scanning and transmission electron micrographs of the clay nanotubes showed the unique hollow structure approximately 50–100 nm in width and an estimated



length in the range of 200–1000 nm (Figures 7A and 7B). TEM micrographs of the interface between RC and the nanotube-modified adhesive are shown in Figures 7C and 7D. Note the presence of small clusters of nanotubes (white arrows).

## Discussion

Over the past decade, the body of work discussing new material- and clinical-based strategies to prolong the durability and overall clinical success of composite restorations through the use of molecules or compounds capable of inhibiting the activity of endogenous proteases has grown exponentially [7–11, 26]. This study provides in-depth details on the loading potential of doxycycline (DOX) onto aluminosilicate nanotubes and its MMP-1 inhibition effects over time upon its release. The results of DOX loading determined by HPLC showed that increased concentrations of DOX significantly amplified the amount of loaded DOX (Table 1). Conversely, higher concentrations of DOX significantly decreased loading efficiency, possibly due to a threshold limit, since the amount of HNT used for loading was constant, regardless of the DOX concentration used. A study conducted by Qi et al. reported a similar trend when HNT was loaded with tetracycline [27]. Since HNT is positively charged on the inner surface and negatively charged on the outer surface, the driving force for drug loading relies on the differences in charge between the cationic DOX [28] and the negatively charged HNT outer surface. Results from Table 1 indicate that part of DOX is absorbed outside of the lumen which is approximately 10% by volume of the tubes and additional loaded DOX may occur in the “pockets” formed between each layer of these multilayer aluminosilicate clay nanotubes due to loose attachment [29]. Moreover when vacuum is applied, DOX may be pushed into the lumen of HNT due to negative pressure, regardless of the charge of the materials.

In terms of physicochemical properties, the modification of the adhesive resin with DOX-loaded nanotubes did not compromise DC (compared within the same curing time, Figure 1) and microhardness (Figure 2) compared to the control ( $p > 0.05$ ). These results suggested that even though DOX incorporation led to a darker adhesive, it did not jeopardize monomer conversion and also the release of DOX was not due to underpolymerized adhesive. Microhardness was performed since it indirectly measures DC on specimens with the same dimensions as those used in the drug release studies to ensure that polymerization of modified adhesives was not affected by specimen thickness. A strong correlation ( $r^2 > 0.9$ ) has been shown to exist between DC and microhardness [30].

The drug release profile showed an initial burst release at day 1, followed by a gradual decrease over time (Figure 3). Even though the release of DOX revealed an initial burst that may not be sustained for long term, clinically, DOX released from the modified adhesive would be localized at the hybrid layer where the active MMPs are present. Interestingly although a higher concentration of DOX ( $> 30\%$ , w/v) could provide the greatest release, the concentration used in this study was limited by solubility and the pH of DOX. Indeed, DOX was not completely dissolved at concentrations higher than 30% (w/v). Moreover, the increased concentration of DOX significantly decreased the pH of the DOX solution (30% DOX pH  $\sim 3.5$  and 50% DOX pH  $\sim 1$ ). Taking into consideration that the pH of the adhesive resin of SBMP is approximately 3.5–4.0, the increased concentration of DOX could lead to a

significant pH drop upon the adhesive's modification, which, in turn, could alter the overall properties of the adhesive or the adhesive/demineralized dentin interactions.

The cumulative release over 28 days was approximately 1–2% of the amount of DOX initially incorporated within the adhesive disks, demonstrating, for the first time, the great potential of Halloysite as a reservoir for loading and sustained release of distinct protease inhibitors. Notably, after long-term storage, the DOX left in the adhesive was approximately 6–13% of the original concentration. In theory, most of the DOX should have either remained in the adhesive or released into the incubation medium. However, a portion of the DOX was lost during incubation. One could argue that there is a possible relationship between the half-life of DOX, which has been reported to be approximately 24 h in vivo or in cell culture conditions [31, 32]. Therefore, it would be beneficial to investigate the effects of other MMP inhibitors such as epigallocatechin gallate or tissue inhibitor of MMPs.

The antimicrobial properties obtained through agar diffusion tests revealed inhibition zones for *S. mutans* and *L. casei* when in contact with the DOX-loaded nanotube-modified adhesives were seen as a function of the amount of DOX within the adhesives (Figure 4). This indicates that DOX was successfully incorporated into the modified adhesive and remained active even after it was processed through the loading testing method used in this study. Most importantly, the eluates prepared from DOX-loaded nanotube-modified adhesives did not inhibit growth of either bacterial strain tested, thus indicating that the concentration of DOX released from the specimens was below MIC for *S. mutans* [0.25–0.50 mg/mL] and *L. casei* [0.38–1.5 mg/mL] [33]. Furthermore, the eluates for all adhesives tested were considered not toxic to hDPSCs ( $p>0.05$ , Figure 5) when compared with the control group (i.e., cells that were not incubated with eluate, 100% survival).

Anti-MMP properties of the experimental DOX-loaded nanotube-modified adhesives were determined based on a FITC-labeled type I collagen assay as the substrate for MMP-1 using the eluates obtained from the adhesives over 28 days. MMP-1 was used since only MMP-1, MMP-8, and MMP-13 are true collagenases and thus cleave fibrillar collagen more efficiently than other MMPs. Furthermore, MMP-1 has also been found in dentin, along with MMP-2, MMP-3, MMP-8, and MMP-9 [34–36]. Overall, DOX-containing eluates from day 1 showed the highest MMP inhibition (16.20–26.33%) and progressively decreased over 28 days (Figure 6). No significant differences in the released DOX among 10% DOX, 20% DOX, and 30% DOX were found at any time point. The degree of MMP-1 inhibition by DOX-containing eluates gradually decreased over time compared to the negative control (Tris buffer). No significant differences in MMP-1 inhibition were found among the 10%, 20%, and 30% DOX groups ( $p>0.05$ ).

The DOX mechanism of inhibition occurs through the chelation of zinc present in the catalytic domain of the MMPs. In this study, native/helical type I collagen derived from rat-tail tendons was used. Worth mentioning, this assay may not provide the true degradation in dentin, because the demineralized dentin may be composed of both denatured and native type I collagen. Moreover, the accessibility of released DOX to bind with MMPs needs to be further investigated. Nevertheless, Toledano et al. (2012) demonstrated that DOX may completely block dentin MMPs for at least 4 weeks [37]. MMPs contain a zinc ion in the

catalytic domain and a non-exchangeable zinc ion that helps to stabilize the MMP structure. Moreover, MMPs also contain 2 or 3 calcium ions. The MMP inhibition of DOX may also occur through the binding of enzyme-associated calcium, thus changing their conformation and eventually resulting in inactivation of the MMPs. This may explain the long lasting and potent inhibition produced by DOX rather than by the sole interaction with the catalytic zinc [38]. Furthermore, DOX may not be suitable for bonded dentin interfaces because MMPs are known to participate in dentin mineralization and it has been previously reported that DOX will inhibit other tissue repair processes [39]. However, what remains is to determine whether this nonselective inhibition of enzymes by zinc/calcium chelators can adversely interfere with the calcification of reparative dentin.

Representative scanning and transmission electron micrographs of the nanotubes are shown in Figures 7A and 7B, respectively. TEM micrographs of the interface between a resin composite and the nanotube-modified adhesive clearly showed the presence of small clusters of nanotubes (Figures 7C and 7D) that was not observed in the control (Figures 7E and 7F), further supporting the hypothesis that nanotubes can be dispersed within the adhesive resin-based matrix and serve as a nanocontainer for drug release, even though this study lacks information regarding immediate and long-term resin-dentin bond durability.

## Conclusions

The current study details the loading potential and MMP inhibition of DOX released from the modified adhesive. Higher DOX led to higher drug loading into HNT and MMP inhibition in a concentration-dependent manner without altering the physicochemical properties of the adhesives and cytotoxicity.

## Acknowledgments

We thank Dr. Bruce Cooper (Bindley Bioscience Center, Purdue University) for assistance with HPLC and mass spectrometry analyses, Dr. Richard L. Gregory (IUSD) for access to his microbiology facilities, and Caroline Miller (Indiana University, School of Medicine) for the TEM study. This manuscript is based on a Dissertation submitted to the graduate faculty, Indiana University Purdue University (IUPUI), in partial fulfillment of the requirements for the Doctor of Philosophy Degree in Dental Sciences.

**Funding** This study was supported in part by a grant from the Delta Dental Foundation (MCB)

## References

1. Ferracane JL. Resin composite--state of the art. *Dent Mater.* 2011; 27:29–38. [PubMed: 21093034]
2. Liu Y, Tjaderhane L, Breschi L, Mazzoni A, Li N, Mao J, Pashley DH, Tay FR. Limitations in bonding to dentin and experimental strategies to prevent bond degradation. *J Dent Res.* 2011; 90:953–968. [PubMed: 21220360]
3. Mjor IA, Moorhead JE, Dahl JE. Reasons for replacement of restorations in permanent teeth in general dental practice. *Int Dent J.* 2000; 50:361–366. [PubMed: 11197194]
4. Van Meerbeek B, De Munck J, Yoshida Y, Inoue S, Vargas M, Vijay P, Van Landuyt K, Lambrechts P, Vanherle G. Buonocore memorial lecture. Adhesion to enamel and dentin: current status and future challenges. *Oper Dent.* 2003; 28:215–235. [PubMed: 12760693]
5. De Munck J, Van Landuyt K, Peumans M, Poitevin A, Lambrechts P, Braem M, Van Meerbeek B. A critical review of the durability of adhesion to tooth tissue: methods and results. *J Dent Res.* 2005; 84:118–132. [PubMed: 15668328]

6. Mazzoni A, Tjaderhane L, Checchi V, Di Lenarda R, Salo T, Tay FR, Pashley DH, Breschi L. Role of Dentin MMPs in Caries Progression and Bond Stability. *J Dent Res*. 2014
7. Breschi L, Martin P, Mazzoni A, Nato F, Carrilho M, Tjaderhane L, Visintini E, Cadenaro M, Tay FR, De Stefano Dorigo E, Pashley DH. Use of a specific MMP-inhibitor (galardin) for preservation of hybrid layer. *Dent Mater*. 2010; 26:571–578. [PubMed: 20299089]
8. Almahdy A, Koller G, Sauro S, Bartsch JW, Sherriff M, Watson TF, Banerjee A. Effects of MMP inhibitors incorporated within dental adhesives. *J Dent Res*. 2012; 91:605–611. [PubMed: 22518030]
9. Carrilho MR, Geraldini S, Tay F, de Goes MF, Carvalho RM, Tjaderhane L, Reis AF, Hebling J, Mazzoni A, Breschi L, Pashley D. In vivo preservation of the hybrid layer by chlorhexidine. *J Dent Res*. 2007; 86:529–533. [PubMed: 17525352]
10. Sartori N, Stolf SC, Silva SB, Lopes GC, Carrilho M. Influence of chlorhexidine digluconate on the clinical performance of adhesive restorations: a 3-year follow-up. *J Dent*. 2013; 41:1188–1195. [PubMed: 24076103]
11. Dutra-Correa M, Saraceni CH, Ciaramicoli MT, Kiyani VH, Queiroz CS. Effect of chlorhexidine on the 18-month clinical performance of two adhesives. *J Adhes Dent*. 2013; 15:287–292. [PubMed: 23560258]
12. Lvov Y, Wang W, Zhang L, Fakhrullin R. Halloysite Clay Nanotubes for Loading and Sustained Release of Functional Compounds. *Adv Mater*. 2016; 28:1227–50. [PubMed: 26438998]
13. Bottino MC, Batarseh G, Palasuk J, Alkhatheeri MS, Windsor LJ, Platt JA. Nanotube-modified dentin adhesive--physicochemical and dentin bonding characterizations. *Dent Mater*. 2013; 29:1158–1165. [PubMed: 24054334]
14. Feitosa SA, Palasuk J, Kamocki K, Geraldini S, Gregory RL, Platt JA, Windsor LJ, Bottino MC. Doxycycline-encapsulated nanotube-modified dentin adhesives. *J Dent Res*. 2014; 93:1270–1276. [PubMed: 25201918]
15. Alkhatheeri MS, Palasuk J, Eckert GJ, Platt JA, Bottino MC. Halloysite nanotube incorporation into adhesive systems--effect on bond strength to human dentin. *Clin Oral Investig*. 2015; 19:1905–1912.
16. Feitosa SA, Munchow EA, Al-Zain AO, Kamocki K, Platt JA, Bottino MC. Synthesis and characterization of novel halloysite-incorporated adhesive resins. *J Dent*. 2015; 43:1316–1322. [PubMed: 26334950]
17. Patel BK, Parikh RH, Aboti PS. Development of oral sustained release rifampicin loaded chitosan nanoparticles by design of experiment. *J Drug Deliv*. 2013; 2013:370938. [PubMed: 24024034]
18. Smith K, Leyden JJ. Safety of doxycycline and minocycline: a systematic review. *Clin Ther*. 2005; 27:1329–1342. [PubMed: 16291409]
19. Palasuk J, Kamocki K, Hippenmeyer L, Platt JA, Spolnik KJ, Gregory RL, Bottino MC. Bimix antimicrobial scaffolds for regenerative endodontics. *J Endod*. 2014; 40:1879–1884. [PubMed: 25201643]
20. International Organization for Standardization ISO 10993-5: biological evaluation of medical devices Part 5: tests for cytotoxicity—in vitro methods. 1993
21. Zhang K, Cheng L, Imazato S, Antonucci JM, Lin NJ, Lin-Gibson S, Bai Y, Xu HH. Effects of dual antibacterial agents MDPB and nano-silver in primer on microcosm biofilm, cytotoxicity and dentine bond properties. *J Dent*. 2013; 41:464–474. [PubMed: 23402889]
22. Birkedal-Hansen H, Yamada S, Windsor J, Poulsen AH, Lyons G, Stetler-Stevenson W, Birkedal-Hansen B. Matrix metalloproteinases. *Curr Protoc Cell Biol*. 2003; (Unit 10):18. Chapter 10.
23. Windsor LJ, Steele DL, LeBlanc SB, Taylor KB. Catalytic domain comparisons of human fibroblast-type collagenase, stromelysin-1, and matrilysin. *Biochim Biophys Acta*. 1997; 1334:261–272. [PubMed: 9101722]
24. Sun J, Song F, Zhang W, Sexton BE, Windsor LJ. Effects of alendronate on human osteoblast-like MG63 cells and matrix metalloproteinases. *Arch Oral Biol*. 2012; 57:728–736. [PubMed: 22251575]
25. Tay FR, Moulding KM, Pashley DH. Distribution of nanofillers from a simplified-step adhesive in acid-conditioned dentin. *J Adhes Dent*. 1999; 1:103–117. [PubMed: 11725676]

26. Montagner AF, Sarkis-Onofre R, Pereira-Cenci T, Cenci MS. MMP Inhibitors on Dentin Stability: A Systematic Review and Meta-analysis. *J Dent Res*. 2014; 93:733–743. [PubMed: 24935066]
27. Qi R, Guo R, Shen M, Cao X, Zhang L, Xu J, Yu J, Shi X. Electrospun poly(lactic-co-glycolic acid)/halloysite nanotube composite nanofibers for drug encapsulation and sustained release. *J Mater Chem*. 2010; 20:10622–10629.
28. Seleem MN, Jain N, Pothayee N, Ranjan A, Riffle JS, Sriranganathan N. Targeting *Brucella melitensis* with polymeric nanoparticles containing streptomycin and doxycycline. *FEMS Microbiol Lett*. 2009; 294:24–31. [PubMed: 19493005]
29. Wei W, Abdullayev E, Hollister A, Mills D, YM L. Clay nanotube/poly(methyl methacrylate) bone cement composites with sustained antibiotic release. *Macromol Mater Eng*. 2012; 297:645–653.
30. Ferracane JL. Correlation between hardness and degree of conversion during the setting reaction of unfilled dental restorative resins. *Dent Mater*. 1985; 1:11–14. [PubMed: 3160625]
31. Centlivre M, Zhou X, Pouw SM, Weijer K, Kleibeuker W, Das AT, Blom B, Seppen J, Berkhout B, Legrand N. Autoregulatory lentiviral vectors allow multiple cycles of doxycycline-inducible gene expression in human hematopoietic cells in vivo. *Gene Ther*. 2010; 17:14–25. [PubMed: 19727135]
32. Strickman D, Sheer T, Salata K, Hershey J, Dasch G, Kelly D, Kuschner R. In vitro effectiveness of azithromycin against doxycycline-resistant and -susceptible strains of *Rickettsia tsutsugamushi*, etiologic agent of scrub typhus. *Antimicrob Agents Chemother*. 1995; 39:2406–2410. [PubMed: 8585717]
33. Al-Ahmad A, Ameen H, Pelz K, Karygianni L, Wittmer A, Anderson AC, Spitzmuller B, Hellwig E. Antibiotic resistance and capacity for biofilm formation of different bacteria isolated from endodontic infections associated with root-filled teeth. *J Endod*. 2014; 40:223–230. [PubMed: 24461408]
34. Wang DY, Zhang L, Fan J, Li F, Ma KQ, Wang P, Chen JH. Matrix metalloproteinases in human sclerotic dentine of attrited molars. *Arch Oral Biol*. 2012; 57:1307–1312. [PubMed: 22608916]
35. van Strijp AJ, Jansen DC, DeGroot J, ten Cate JM, Everts V. Host-derived proteinases and degradation of dentine collagen in situ. *Caries Res*. 2003; 37:58–65. [PubMed: 12566641]
36. Sulkala M, Tervahartiala T, Sorsa T, Larmas M, Salo T, Tjaderhane L. Matrix metalloproteinase-8 (MMP-8) is the major collagenase in human dentin. *Arch Oral Biol*. 2007; 52:121–127. [PubMed: 17045563]
37. Toledano M, Yamauti M, Osorio E, Osorio R. Zinc-inhibited MMP-mediated collagen degradation after different dentine demineralization procedures. *Caries Res*. 2012; 46:201–7. [PubMed: 22516944]
38. Smith GN Jr, Mickler EA, Hasty KA, Brandt KD. Specificity of inhibition of matrix metalloproteinase activity by doxycycline: relationship to structure of the enzyme. *Arthritis Rheum*. 1999; 42:1140–6. [PubMed: 10366106]
39. Beekman B, Verzijl N, de Roos JA, Koopman JL, TeKoppele JM. Doxycycline inhibits collagen synthesis by bovine chondrocytes cultured in alginate. *Biochem Biophys Res Commun*. 1997; 237:107–10. [PubMed: 9266839]

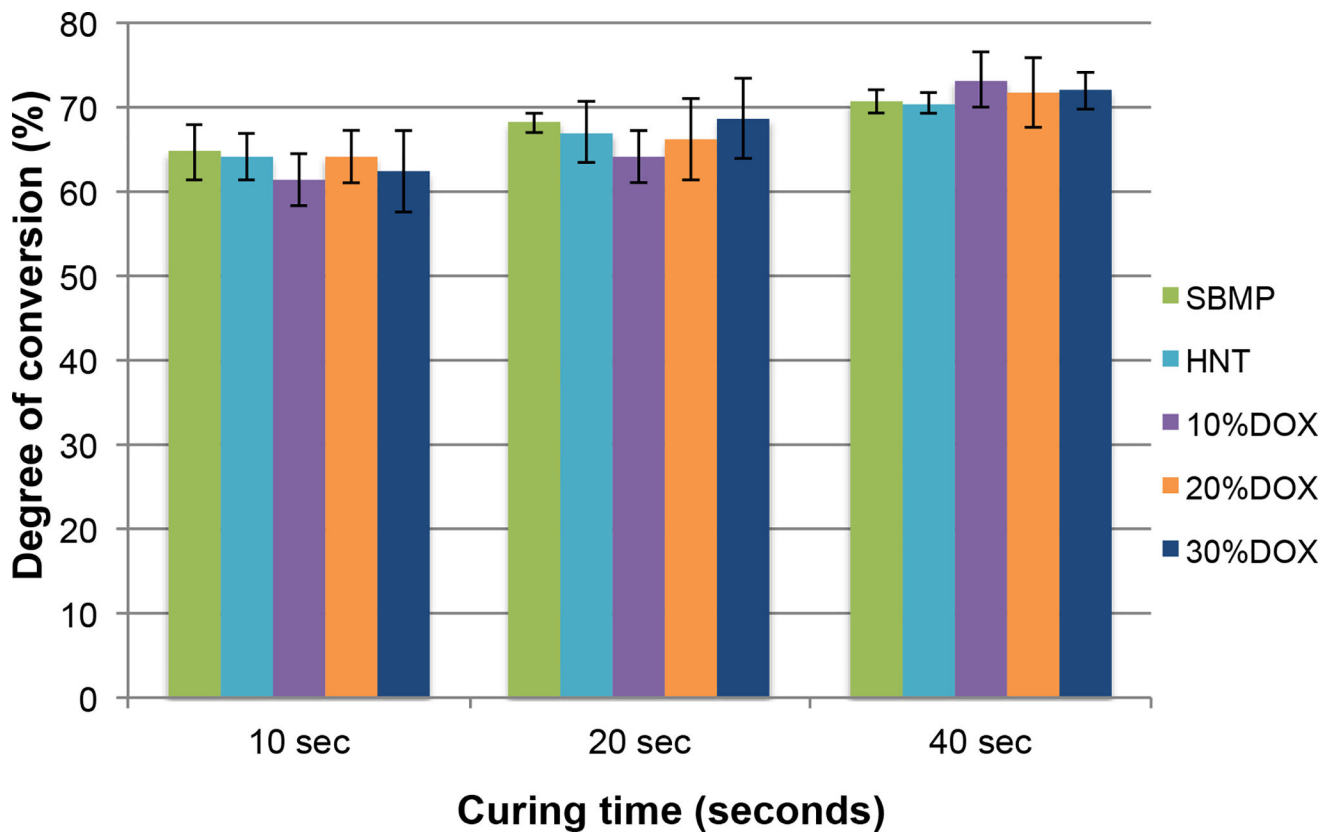


**Figure 1.**

Degree of conversion (DC) of the control (SBMP) and modified adhesives that were light-cured for 10, 20 or 40 sec. Increased curing times led to an increase in the DC values: 61.40–64.68% (10 sec), 64.15–68.65% (20 sec), and 70.44–73.26% (40 sec). No significant differences were found in DC (with each curing time) among the groups ( $p>0.05$ ).

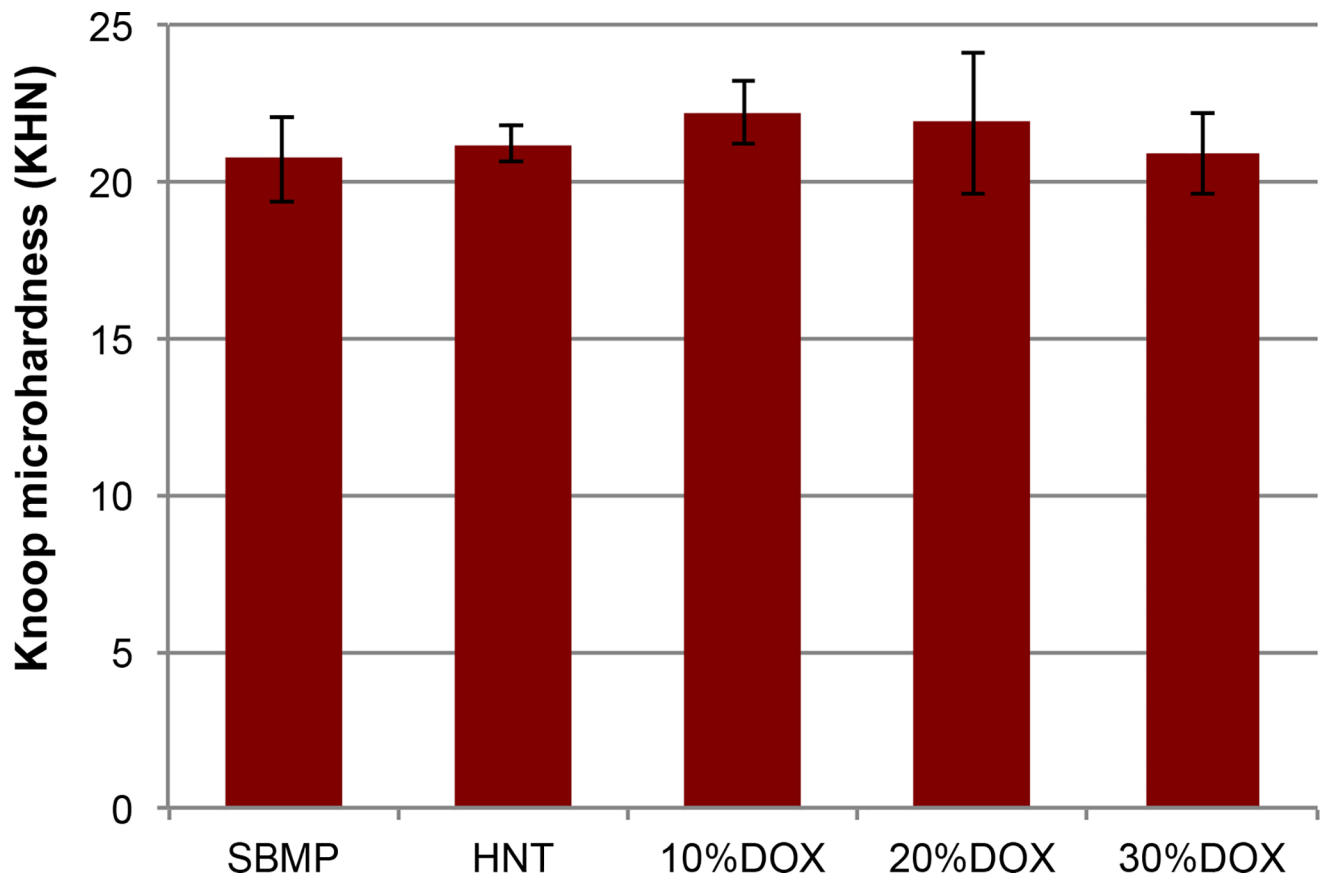


**Figure 2.** Knoop microhardness number (KHN) of the control (SBMP) and modified adhesives polymerized for 20 sec. KHN was  $20.72 \pm 1.38$  (SBMP),  $21.21 \pm 0.59$  (HNT),  $22.18 \pm 0.97$  (10% DOX),  $21.87 \pm 2.28$  (20% DOX), and  $20.89 \pm 1.30$  (30% DOX). No significant differences were found in Knoop microhardness among the groups ( $p > 0.05$ ).

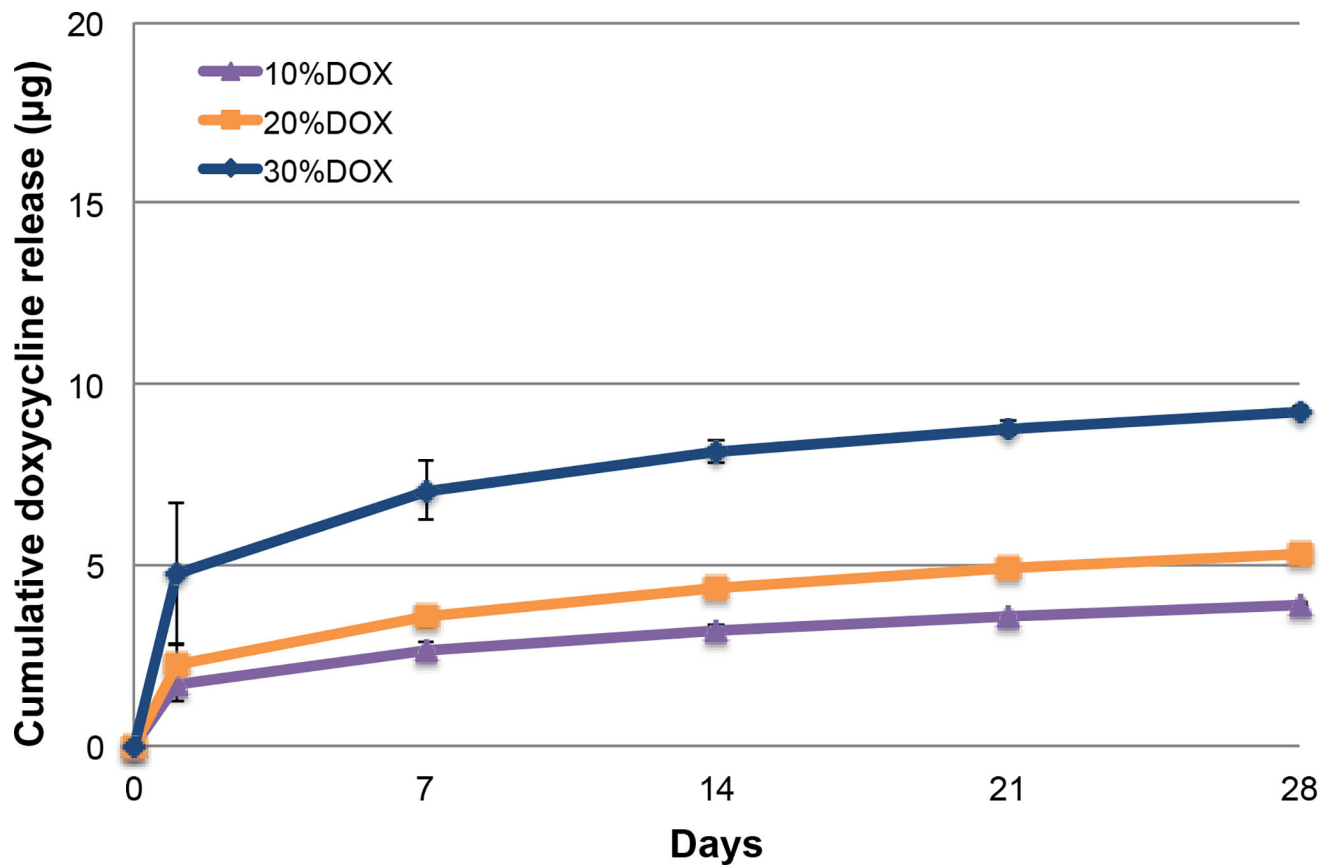


**Figure 3.** Cumulative release profile ( $\mu\text{g}$ , mean  $\pm$  SE) of the control (SBMP) and modified adhesives determined by mass spectrometry. No significant differences in total cumulative DOX release were found among 10%, 20%, and 30% DOX ( $p = 0.259$ ).



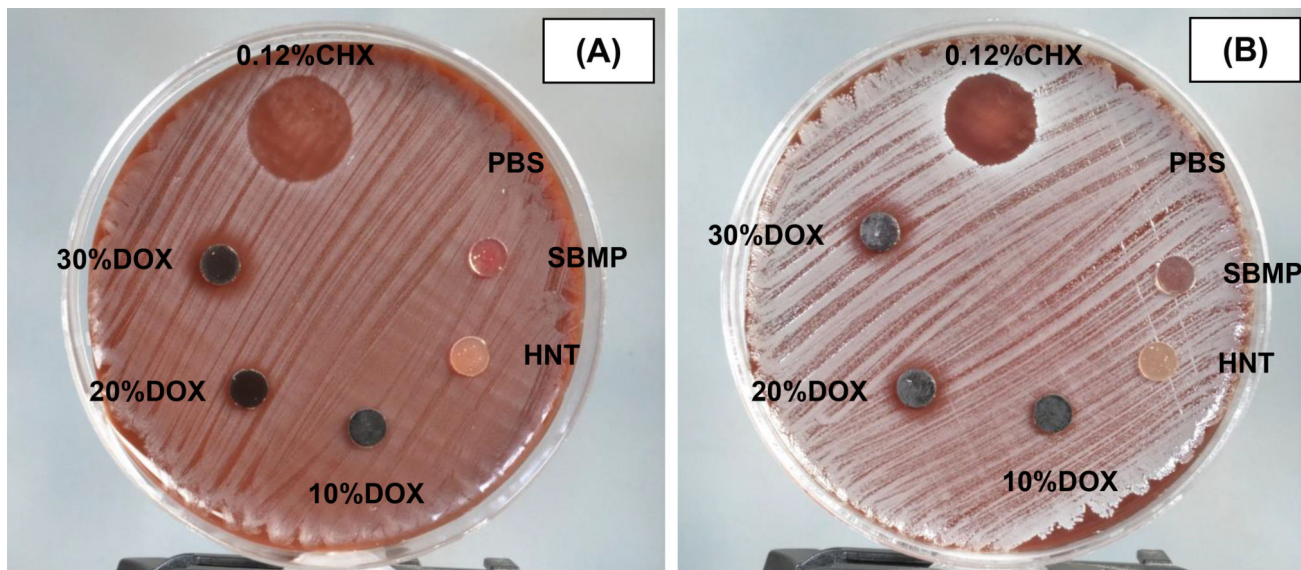


**Figure 4.**

Representative images of agar diffusion data of the control (SBMP) and modified adhesive disks against *S. mutans* (A) and *L. casei* (B) after 72 h of incubation. The average inhibition zones on *S. mutans* were  $16.0 \pm 1.1$  mm (0.12% chlorhexidine, CHX),  $2.3 \pm 3.6$  mm (10% DOX),  $8.1 \pm 0.9$  mm (20% DOX), and  $11.5 \pm 2.6$  mm (30% DOX). The average inhibition zones on *L. casei* were  $14.4 \pm 0.5$  mm (0.12% chlorhexidine),  $5.1 \pm 4.0$  mm (10% DOX),  $7.2 \pm 3.7$  mm (20% DOX), and  $11.3 \pm 1.8$  mm (30% DOX). 0.12% CHX and sterile PBS, served as the positive and negative controls, respectively. No inhibition zones were observed with specimen disks of SBMP, HNT, sterile PBS and DOX-containing eluates of all groups (data not shown). Statistical analysis showed that the inhibition zones on *S. mutans* and *L. casei* were statistically significant among 10%DOX, 20%DOX, and 30%DOX, except for the inhibition zone of *L. casei*, which was between 10%DOX and 20%DOX.

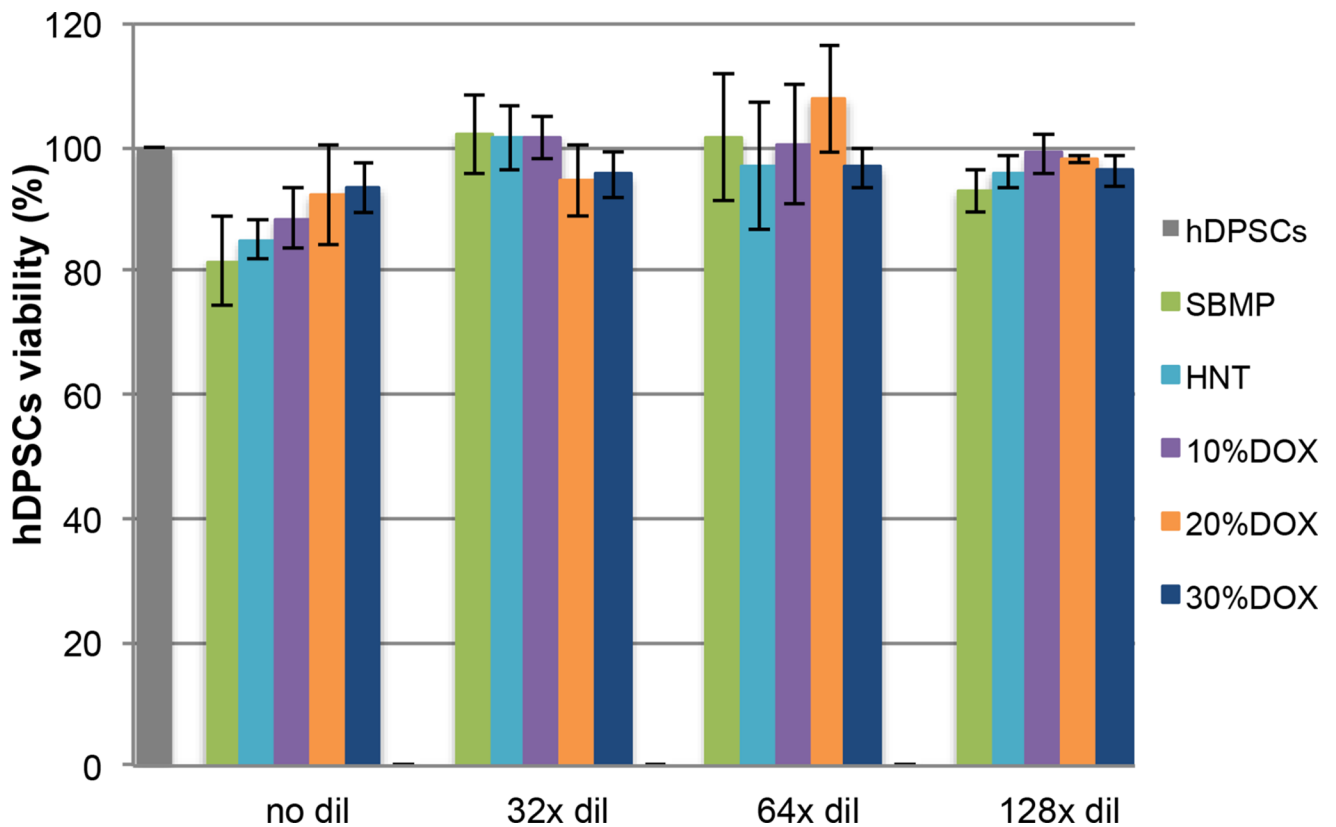


**Figure 5.**

Viability of human dental pulp stem cells (hDPSCs, %). hDPSCs were exposed to eluates of the control (SBMP) and modified adhesive disks. Viability of the cells incubated with various eluates ranged from 81.60% to 107.92% compared to that of the cells not incubated with eluate (100% survival). No significant differences were found among cells incubated with eluates of the same dilution of each group of samples, compared with cells not incubated with eluates.

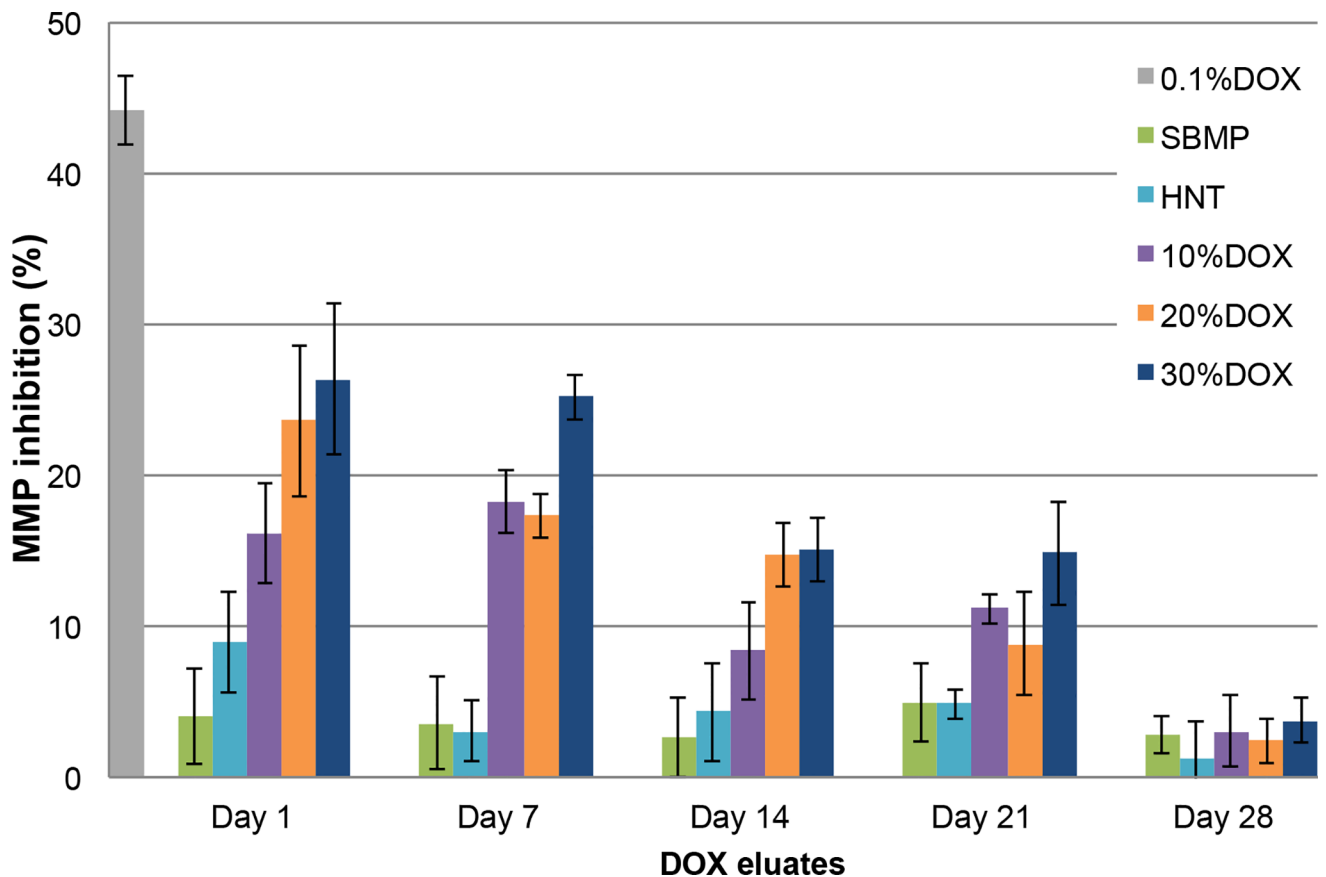


**Figure 6.**

Inhibition of MMP-1 by DOX-containing eluates (% , mean  $\pm$  SE) compared to the negative control (Tris buffer). MMP-1 inhibition was gradually diminished over time. Statistical analysis showed a significant difference between 0.1% DOX and each of the samples from various time points. At day 1, eluates of 30% DOX showed significantly higher MMP inhibition than those of the control (SBMP,  $p < 0.05$ ). At day 7, eluates of 10% and 30% DOX showed significantly higher MMP inhibition than those of control (SBMP) and HNT ( $p < 0.05$ ). No other significant differences in MMP-1 inhibition were found among other eluates ( $p > 0.05$ ).

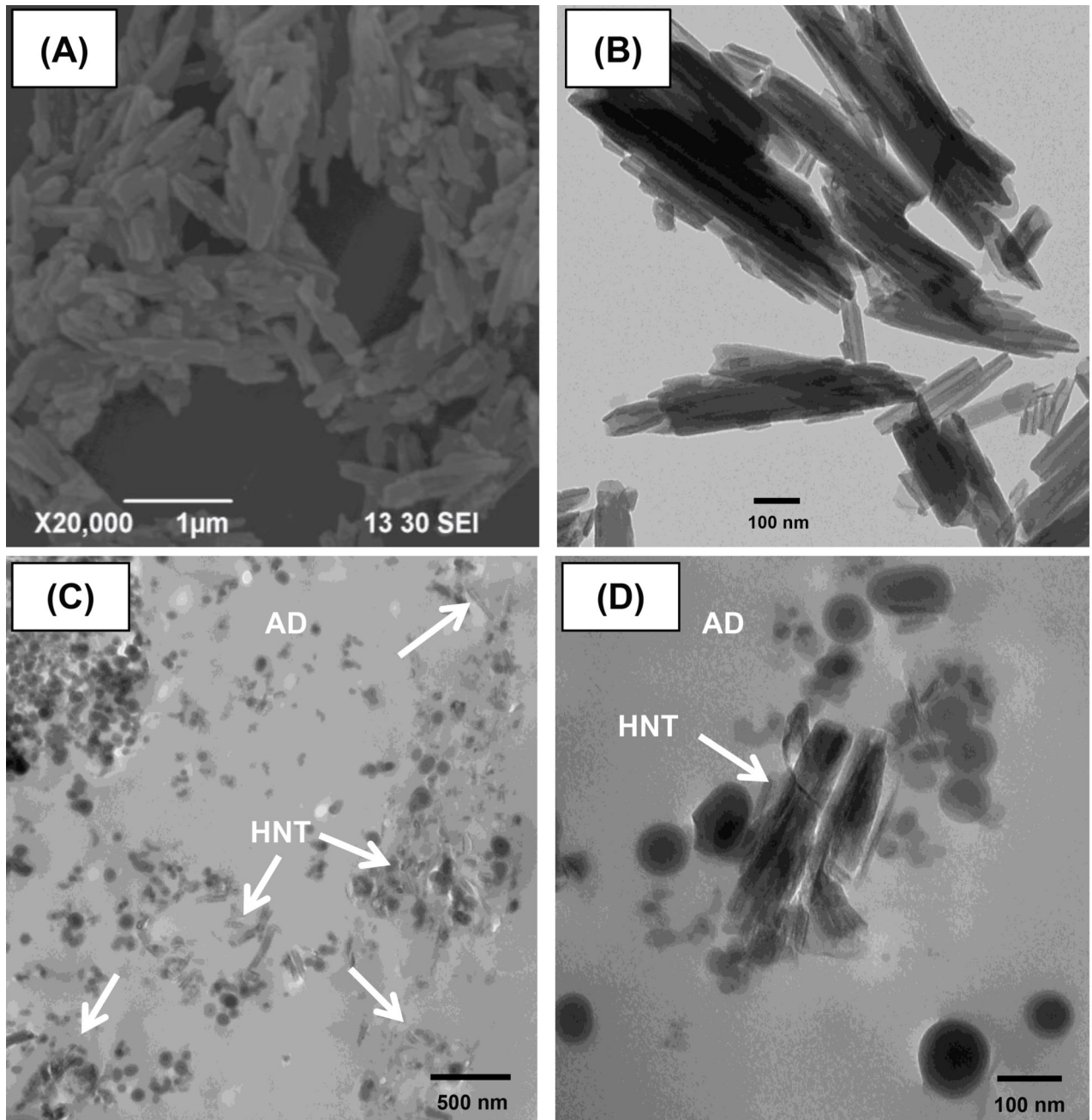


**Figure 7.** Scanning (A) and transmission (B) electron micrographs at 20,000× and 68,000×, respectively of the nanotubes (HNT, white arrows) used. TEM micrographs of the interface between resin composite (RC) and HNT-modified adhesive at 20,000× (C) and 120,000× (D).

**Table 1**

Encapsulation of doxycycline (DOX) determined by HPLC.

Group	Loaded DOX (g)	Loading Efficiency (%)	Drug Loading* (%)
10% DOX	0.24 ± 0.00	47.48 ± 1.68	19.00 ± 0.00
20% DOX	0.36 ± 0.01	36.24 ± 0.54	29.00 ± 0.00
30% DOX	0.47 ± 0.02	31.54 ± 1.05	38.00 ± 0.01

\* Drug loading (DOX:HNT) is the ratio between loaded DOX and added HNT (1.25 g).

Author Manuscript

Author Manuscript

Author Manuscript

Author Manuscript